ACCURATE SEGMENTATION METHOD FOR ROADSIDE LAMPPOSTS BASED ON VEHICLE-MOUNTED LIDAR POINT CLOUDS

Dengfeng Li[1], Yaoyu Li[2], Yuhang Fan[2], Shengjun Tang[2] *

[1] China communications information
technology group co., ltd., Beijing, China
-(lidengfeng1@ccccltd.cn)
[2] School of Architecture and Urban Planning, Research Institute for Smart Cities, Shenzhen University, Shenzhen, China
- liyaoyuvers@163.com, fanyuhang@email.szu.edu.cn, shengjuntang@szu.edu.cn

KEY WORDS: MLS point cloud,street lamp extraction, individual extraction, principal component analysis, supervoxel clustering

ABSTRACT:

The extraction of roadside lampposts constitutes a significant research focus within the domain of vehicular LiDAR point cloud object retrieval. Addressing the complexities inherent in discerning lampposts amidst convoluted vegetation in diverse roadway settings, this study introduces an innovative, progressive technique for the individualized extraction of lampposts utilizing vehicular LiDAR point clouds. The proposed method initiates with a bifurcation of the primary point cloud into terrestrial and aerial subsets via the Cloth Simulation Filter (CSF) algorithm. Subsequent processes involve the extraction of distinct lamppost structures from aerial point clouds through a methodology integrating elevation-normalized spatial partitioning and directional coverage analysis, thereby facilitating precise lamppost localization. The culmination of this process involves the refinement of lamppost point clouds through supervoxel clustering complemented by a non-discretization filter grounded in Principal Component Analysis (PCA). The efficacy of this novel approach is substantiated through empirical studies employing a LiDAR dataset encompassing extensive adhesive scenarios, whereupon comparative analysis with extant methodologies reveals its enhanced proficiency in isolating individual lampposts in complex environments.

1. INTRODUCTION

The digitization of traffic infrastructure emerges as a foundational element in the establishment of a comprehensive, interconnected, scenario-encompassing, and intelligent urban traffic system, with streetlights being a vital component. Their role in intelligent traffic systems underscores the necessity for swift acquisition of streetlight attribute information, a critical demand in the evolution of urban traffic systems towards smart and digital modalities (Yu et al., 2014, Wu et al., 2016, Vaaja et al., 2015).

The acquisition of streetlight data predominantly employs methodologies like manual measurement, 3D photogrammetry, and LiDAR (Light Detection And Ranging) scanning(Wang, 2013, Qin and Gruen, 2021) However, manual measurements, hindered by safety and efficiency concerns, are progressively diminishing in use. Photogrammetry, which relies on semi-automated interpretation of remote sensing imagery to extract three-dimensional geographic information of road elements, offers enhanced efficiency but is constrained by external factors, such as lighting conditions. In contrast, 3D LiDAR technology, characterized by its high-frequency, rapid laser scanning capabilities, captures extensive, high-resolution 3D data in a non-invasive manner, thus standing out as a preferred approach for rapid urban road data acquisition. Specifically, Mobile Laser Scanning (MLS), a specialized LiDAR variant, demonstrates exceptional efficiency, accuracy, and resilience to interference, and is increasingly recognized as a crucial tool for urban road data collection. Nonetheless, the intricate urban road environment, particularly the frequent overlapping of streetlights with nearby vegetation, poses significant challenges in their identification and extraction. Consequently, refining methods for accurate and comprehensive extraction of streetlight point clouds from MLS data remains an imperative research focus.

Recent research trends in MLS-based streetlight extraction have diversified, predominantly categorizing into model-based, feature-based, and machine learning approaches. Model-based strategies, exemplified by the dual-cylinder model, focus on identifying streetlight poles, followed by individualized extraction of man-made pole-like structures through techniques such as region growing(Li et al., 2016, Kang et al., 2018, Shi et al., 2018). Despite their general effectiveness, these methods are susceptible to interference from nearby tree trunks and demonstrate limited accuracy in scenarios where streetlights and trees overlap. Feature-based methods, analyzing point cloud geometrical and spatial attributes, construct classification features to facilitate individualized extraction (Yang et al., 2018, Liu et al., 2020, Huang and You, 2016). While this approach mitigates tree trunk interference, it encounters substantial classification errors in scenarios of extensive streetlight-vegetation overlap, leading to potential misidentification. Machine learning-based methods, leveraging annotated datasets for model training, offer efficient extraction capabilities(Yadav et al., 2022, Li et al., 2018). However, the time-intensive nature of manual annotation and the need for improved accuracy in complex adhesive scenarios highlight the limitations of this approach.

Overall, current methodologies predominantly focus on extracting streetlights characterized by clear spatial independence. In scenarios of overlapping streetlights and vegetation, these techniques often misidentify streetlights as other objects, incorporating extensive vegetation data in the extraction results, thereby diminishing accuracy in complex road environments. Addressing this challenge, this paper introduces a progressive MLS-

* Corresponding author

based method for the individualized extraction of streetlights. Illustrated in Figure 1, the method initiates with the preprocessing of original MLS point clouds through statistical and cloth simulation filtering. It then advances to extract streetlight poles from non-ground point clouds via elevation-normalized spatial segmentation, voxel region growth based on convex hull area rate change, and spatial range coverage analysis, achieving precise streetlight localization and recognition. Ultimately, the method, integrating supervoxel clustering and Principal Component Analysis, accomplishes the individualized extraction of streetlight point clouds, marking a significant advancement in the field.

2. INDIVIDUAL STREETLIGHT EXTRACTION

2.1 Point Cloud Preprocessing

Given the operational principles of mobile laser scanning devices, the collected MLS point clouds typically contain a substantial amount of scattered noise points. Moreover, in MLS point clouds, ground points occupy a significant portion of storage space and amalgamate points from various objects into a single set, which complicates the individual extraction process of streetlights. Consequently, this paper employs statistical filtering and the Cloth Simulation Filter (CSF) proposed by Zhang et al.(Zhang et al., 2016) to remove noise and ground points from the original data.

2.2 Streetlight Localization

The typical road environment containing streetlights often includes numerous interfering objects such as street trees, buildings, and vehicles, making it challenging to directly extract streetlight point clouds from the original data. To address this, the study first utilizes spatial elevation slicing to obtain a point cloud slice primarily comprising streetlight poles. Subsequently, the pole point clouds are extracted, providing crucial localization information for streetlights and serving as the basis for subsequent individualized extraction.

Spatial Segmentation Based on Elevation Normalization: Due to potential variations in road surface heights, especially in terrains with significant undulations, using a uniform elevation threshold for point cloud filtering may result in the omission of many lampposts, thereby impeding accurate streetlight localization. To counter this, the study normalizes non-ground point clouds to a common elevation plane prior to spatial elevation segmentation, mitigating the impact of terrain undulations on the results. Elevation Normalization: Utilizing the ground point clouds obtained from preprocessing, the study employs inverse distance weighted interpolation (Formulas 1 and 2) to interpolate these points and create a Digital Elevation Model (DEM). Following this, the non-ground point clouds are subtracted from the DEM elevation (as per Formula 3) to align them on a consistent horizontal plane.

$$Z = \frac{\sum_{i=1}^{n} \frac{Z_i}{P_i}}{\sum_{i=1}^{n} \frac{1}{P_i}} \tag{1}$$

$$P_i = \left((X - X_i)^2 + (Y - Y_i)^2\right)^{\frac{q}{2}} \tag{2}$$

$$Z_{i,deter} = Z_i - Z_{grid} \tag{3}$$

Where X, Y are the coordinates of the interpolation point, X_i, Y_i are the coordinates of the neighboring points, P_i represents the weight, q is the power, i is the index of the neighboring points, n is the number of neighboring points within the search area, $Z_{i,deter}$ is the normalized elevation value of any non-ground point, Z_i is the original elevation value of the point, and Z_{grid} is the corresponding elevation value of the DEM grid where the point is located.

Spatial Elevation Segmentation: Identify the lowest elevation value of the non-ground point cloud after elevation normalization, and set an elevation threshold. As shown in Figure 1, based on elevation filtering, spatially segment the non-ground point cloud within the elevation range to obtain a slice point cloud that includes the streetlight poles.

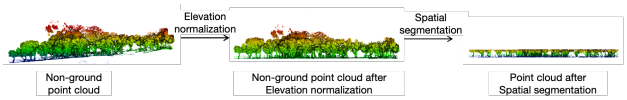

Figure 1. The workflow of elevation-normalized spatial segmentation.

Extraction of Streetlight Poles Based on Voxel Region Growth and Spatial Range Coverage Analysis: After acquiring the slice point cloud, the next step is to extract the pole point cloud for streetlight localization. In this study, we employed the voxel region growth algorithm based on the rate of change in convex hull area that we previously proposed by(Wang et al., 2023) to extract potential candidate point cloud clusters that may represent lampposts. However, these candidate clusters often include many tree trunks from street trees, necessitating further differentiation to eliminate interference. Existing studies typically distinguish between lampposts and tree trunks by analyzing the spatial distribution characteristics of neighboring point clouds around the lampposts, but this presupposes that the tops of the streetlights do not overlap with surrounding vegetation. Nevertheless, in extensive adhesive scenarios, the tops of the lights often overlap with surrounding vegetation, making it difficult for existing methods to differentiate between the two using traditional approaches.

To address the issue of identifying streetlight poles in extensive adhesive scenarios, this paper proposes a method of spatial orientation coverage analysis, which operates as follows:

(1) Calculate the centroid of the candidate streetlight pole point cloud cluster. Then, use this centroid as the center of a circle with a specified radius to perform cylindrical filtering within the non-ground point cloud, retaining only those points that are higher than the candidate streetlight pole point cloud cluster.

(2) As shown in Figure 4, use the specified radius to layer the cylindrical point cloud in the XY dimension, resulting in multiple annular point clouds that exclude the top region of the pole structure. Red arrows originating from the center divide the point cloud into eight spatial azimuthal sectors. For each layer of annular point clouds, calculate the coverage value for each azimuthal sector according to Formula 4 to represent the spatial coverage situation, as illustrated in Figure 2. Here, A_{ring} denotes the horizontal convex hull area of the annular point cloud within the azimuthal sector range, and A_{sector} denotes the area of the annular sector within the azimuthal range. If $A_{ring} \geq A_{sector}$ for the k-th annular layer in the XY dimension, it is considered to cover the j-th azimuthal sector; other-

wise, it does not cover. After completing the azimuthal coverage analysis for all annular layers, use Formula 5 to calculate the coverage value for each azimuthal sector of the entire annular structure, where C_{sector} represents the coverage value of the annular structure in the j-th azimuthal sector.

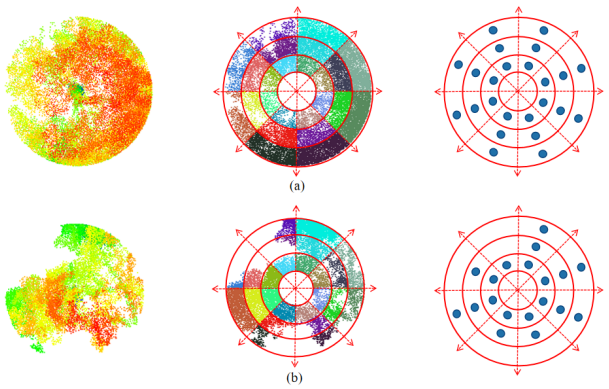

Figure 2. Principle diagram of spatial orientation coverage analysis: (a) Roadside trees, (b) Overlapping artificial poles.

$$AC_i^k = \{1 \; if \frac{S_{CH}}{S_{Sector}} \geq 0.70 otherwise \tag{4}$$

$$AC_i = \frac{1}{n}\sum_{k=1}^{n} AC_i^k \tag{5}$$

(3) As shown in Formula 6, if more than half of the azimuthal sectors of the annular layers have a coverage value of 1, and the number of such layers is more than 4, then the candidate pole point cloud cluster is considered a streetlight pole. Specifically, if $AC_i^j = 1$ for more than half of the azimuthal sectors, and if $SY \geq 2$ for the number of annular layers with such a condition, then the candidate point cloud cluster is deemed to be that of a streetlight pole, and the process proceeds to the next step; otherwise, it is discarded.

$$AC_i = \frac{1}{n}\sum_{k=1}^{n} AC_i^k \tag{6}$$

2.3 Individualized Extraction of Streetlights

The localization information of streetlights is essential for their individualized extraction. However, in extensive adhesive scenarios, streetlights are often surrounded by vegetation such as tree canopies, and using mainstream extraction methods like graph cut or region growing could result in the inclusion of a substantial amount of vegetation in the point cloud, thus reducing the extraction accuracy. To address this issue, building upon the point cloud classification method based on supervoxels proposed by Li et al.(Li et al., 2018), this paper introduces an individualized extraction method based on supervoxel clustering and Principal Component Analysis (PCA).

Supervoxel Clustering: As shown in Figure 3, the VCCS (Voxel Cloud Connectivity Segmentation) method is initially applied to the cylindrical point cloud obtained during the localization process to perform supervoxel segmentation, achieving a preliminary separation of vegetation and streetlight point clouds. Subsequently, clustering of the supervoxel point cloud is conducted using constraints such as Euclidean distance and the angle between normal vectors of point clouds to mitigate the interference of supervoxel oversegmentation on the local geometric characteristics of the point clouds.

The algorithmic procedure for supervoxel clustering is as follows: (1) Select the supervoxel with the smallest distance to the

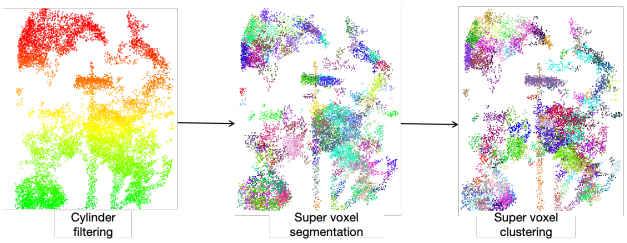

Figure 3. Flowchart of super-voxel clustering.

centroid of the cylindrical point cloud as the seed supervoxel SV_{seed}. (2) Search for the k nearest supervoxels to SV_{seed}, denoted as $SV_1, ..., SV_k$. (3) For each candidate supervoxel $SV_i, i = 1, ..., k$, calculate the angle with SV_{seed} based on their normal vectors, referred to as $Angle_{normal}$. If the angle meets the criteria, merge SV_i into the target cluster T_p, which consists of supervoxels with similar orientation. (4) Repeat the process until all supervoxels have been processed.

The Chinese text provided discusses the use of Principal Component Analysis (PCA) for vertical judgment in the context of point cloud data processing for streetlight poles. Here’s the academically styled translation in English:

Vertical Judgment Based on Principal Component Analysis: Due to the fact that the pole point clouds obtained from the localization are typically derived from slice point clouds and are not completely intact, it is necessary to further extract from the clustered supervoxels.

Initially, Principal Component Analysis is employed to calculate the eigenvalues of all clustered supervoxels. Each clustered supervoxel’s linearity, planarity, and volumetric features are determined based on eigenvalues according to Formula 7,8,9. The most prominent feature corresponding to the maximum eigenvalue is then selected to represent the spatial geometric characteristic of that supervoxel.Then, for all linear supervoxels, calculate the distance between their centroids and the centroid of the pole point cloud obtained from the localization on the XY plane. If this distance is less than 0.3, and the angle between the principal direction vector of the supervoxel and the principal direction vector of the pole point cloud obtained from localization is less than 15 degrees or greater than 85 degrees, then merge it with the pole point cloud obtained from the localization to acquire a complete point cloud of the streetlight pole.

$$q_L = \sqrt{\lambda_1} - \sqrt{\lambda_2}/\sqrt{\lambda_1} \tag{7}$$

$$q_P = \sqrt{\lambda_2} - \sqrt{\lambda_3}/\sqrt{\lambda_1} \tag{8}$$

$$q_V = \sqrt{\lambda_3}/\sqrt{\lambda_1} \tag{9}$$

Non-discreteness Filtering Based on Principal Component Analysis: Following the extraction of the streetlight pole, it is

necessary to extract the non-pole parts of the streetlight point cloud. Compared to the non-pole parts of streetlights, vegetation point clouds typically exhibit a random and dispersed nature. Therefore, as shown in Figure 4, this paper employs the non-discreteness filtering method proposed by Li et al. (Li et al., 2022)to remove tree crowns present in the remaining planar and volumetric supervoxels. The non-discreteness feature value of each planar or volumetric supervoxel is calculated according to Formula 10. If it is less than a specified threshold, the supervoxel is considered to be part of the vegetation point cloud.

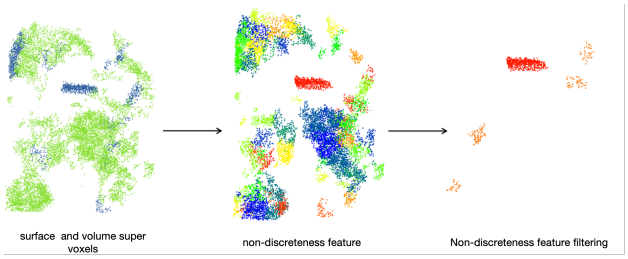

Figure 4. Flowchart of non-discrete filtering.

$$P_{sc}(P) = 1 - \sqrt[1/3]{\lambda_1 * \lambda_2 * \lambda_3} \tag{10}$$

To further enhance the extraction precision and to mitigate the impact of residual tree crowns remaining after non-discreteness filtering on the final results, the supervoxel point cloud post-filtering is subjected to stretching of the minimum bounding rectangle, with increases in length and width by DL and DW respectively. If the stretched bounding rectangle encompasses the centroid of the complete pole point cloud, then the supervoxel is considered to be part of the non-pole section of the streetlight. Merging all supervoxels that meet the above criteria yields the point cloud of the non-pole sections of the streetlight.

3. EXPERIMENT

3.1 Data preparation and accuracy evaluation

To validate the effectiveness of the method proposed in this paper, as illustrated in Figure 5, this study employs the aforementioned MLS point cloud dataset to conduct both qualitative and quantitative assessments of the introduced technique.

This dataset was collected using a backpack-mounted laser scanner and represents a portion of the Shenzhen University campus roads. It is characterized by the presence of numerous streetlights entangled with surrounding vegetation within the dataset. Consequently, this dataset effectively validates the method’s ability to individually extract entangled man-made pole-like objects. Table 1 displays the basic information of the dataset.

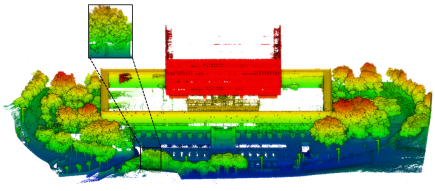

Figure 5. Visulization of the dataset.

Count	Density/m3	Road lengthm	Lamp number
91,237,947	2358	403	20

Table 1. Description of datasets

In terms of quantitative analysis, this paper uses recall ($Recall$) and precision ($Precision$) as detection evaluation metrics. Their calculation methods are shown in Formula 11 and 12, where TP represents true positives, FP represents false positives, and FN represents false negatives. Recall measures completeness or quantity, while precision measures accuracy or quality.

$$Recall = \frac{TP}{TP + FN} \tag{11}$$

$$Precision = \frac{TP}{TP + FP} \tag{12}$$

3.2 Experimental Results and Accuracy Analysis

The overall experimental process begins with preprocessing the experimental dataset using statistical filtering and cloth filtering. Subsequently, lamp post localization is achieved through elevation-normalized spatial segmentation, voxel region growing, and spatial orientation coverage analysis. Finally, lamp post point cloud individualization is accomplished based on the localization information, utilizing super-voxel clustering, vertical determination, and non-discrete filtering. The specific experimental results on this dataset are illustrated in Figure 6. Regarding algorithm parameters, the following values were used: a neighborhood size of 30 for calculating the standard deviation in statistical filtering, a standard deviation multiple of 1.0, an interpolation grid resolution of 0.05m for DEM generation, distance threshold for spatial segmentation, cylinder filtering radius for spatial orientation coverage analysis, normal vector angle threshold for super-voxel clustering, non-discrete filtering threshold, and stretching length of the minimum bounding rectangle. In Figure 6, the red border represents the positions of the lamp posts in this dataset, while the black dashed border indicates lamp post extraction errors and omissions due to localization errors. To further analyze the superiority of

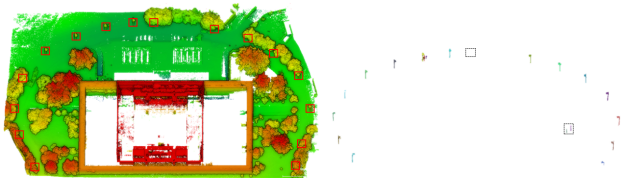

Figure 6. Experimental results of lamp post individualization in the dataset.

our method, we also selected two different and representative lamp post individualization methods, the Rand_La Net(Hu et al., 2020) method and the method based on dual-cylinder models(Kang et al., 2018), to extract and compare the lamp posts that overlap with the surrounding vegetation in the experimental dataset. Figure 7 and Tables 2 present the results of lamp post individualization for our method and the two comparative methods, along with their corresponding precision and recall rates.

As shown in Figure 7 and Tables 2, when dealing with heavily adhesive and overlapping scenes, our method often produces the best extraction results among the three methods, with precision and recall rates generally above 90%. When considering missed detections, our method achieves an average precision

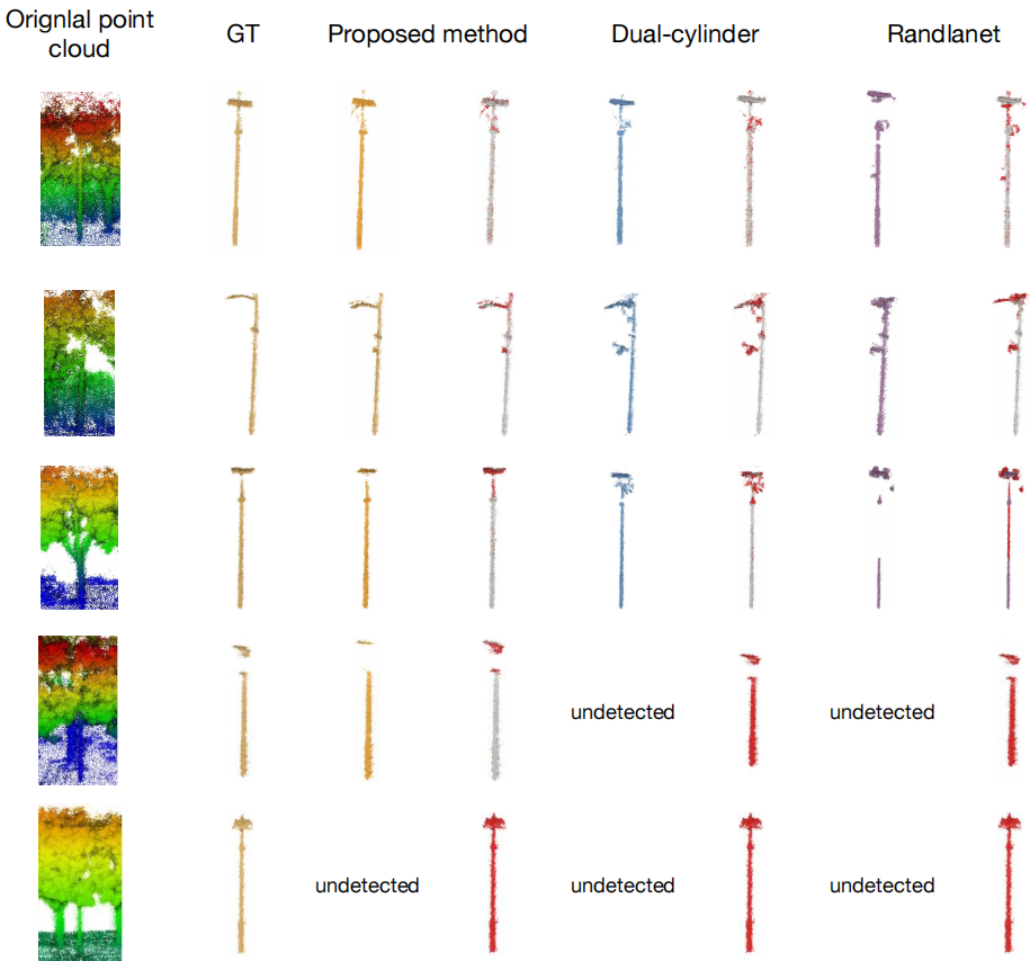

Figure 7. Experimental results of lamp post individualization in the dataset.

Metrics	method	Index										Average
		1	2	3	4	5	6	7	8	9	10	
3*Pr	proposed	97.84	91.29	97.79	99.59	0.0	93.21	94.77	99.84	93.08	95.45	90.32
	dual-cylinder	93.57	73.25	82.60	0.00	0.00	70.86	58.21	90.17	82.99	75.26	62.69
	randlanet	91.36	73.28	70.96	0.00	0.00	0.00	46.22	98.40	66.79	89.14	53.62
3*Re	proposed	98.94	92.24	83.71	87.75	0.00	98.70	96.35	97.80	94.39	83.51	82.95
	dual-cylinder	94.85	92.02	88.03	0.00	0.00	98.64	89.69	99.82	78.89	79.00	72.10
	randlanet	97.51	81.25	66.35	0.00	0.00	0.00	87.53	98.58	71.41	90.9	59.33

Table 2. The quantitative comparison of lamp post individualization results (Red indicates the best performance).

and recall rate of over 80%. In comparison, the dual-cylinder method and Rand_La Net method both have average precision and recall rates of around or below 70%. Therefore, it can be concluded that the method proposed in this paper achieves superior lamp post individualization results in scenarios with extensive adhesion compared to existing mainstream methods.

4. CONCLUSIONS

This paper proposes a precise segmentation method for streetlights based on MLS point clouds. The method begins with preprocessing the original point cloud using statistical filtering and cloth filtering. It then proceeds to perform streetlight localization through elevation-based spatial segmentation, voxel region growth, and spatial coverage analysis. Finally, using the localization information, it achieves precise individualization of streetlight point clouds through super-voxel clustering, vertical determination based on principal component analysis, and non-discretization filtering.

To validate the effectiveness of the proposed method, the paper utilizes an MLS point cloud dataset containing extensive scenarios with heavy adhesion for experimental verification and precision analysis. The experimental results demonstrate that this method is capable of effectively extracting streetlight targets in scenarios with extensive adhesion. Furthermore, when compared to other existing methods, the proposed method consistently achieves superior results in streetlight individualization.

REFERENCES

Hu, Q., Yang, B., Xie, L., Rosa, S., Guo, Y., Wang, Z., Trigoni, N., Markham, A., 2020. Randla-net: Efficient semantic segmentation of large-scale point clouds. *Proceedings of the IEEE/CVF conference on computer vision and pattern recognition*, 11108–11117.

Huang, J., You, S., 2016. Point cloud labeling using 3d convolutional neural network. *2016 23rd International Conference on Pattern Recognition (ICPR)*, IEEE, 2670–2675.

Kang, Z., Yang, J., Zhong, R., Wu, Y., Shi, Z., Lindenbergh, R., 2018. Voxel-based extraction and classification of 3-D pole-like objects from mobile LiDAR point cloud data. *IEEE Journal of Selected Topics in Applied Earth Observations and Remote Sensing*, 11(11), 4287–4298.

Li, F., Oude Elberink, S., Vosselman, G., 2018. Pole-like road furniture detection and decomposition in mobile laser scanning data based on spatial relations. *Remote sensing*, 10(4), 531.

Li, J., Cheng, X., Xiao, Z., 2022. A branch-trunk-constrained hierarchical clustering method for street trees individual extraction from mobile laser scanning point clouds. *Measurement*, 189, 110440.

Li, L., Li, Y., Li, D., 2016. A method based on an adaptive radius cylinder model for detecting pole-like objects in mobile laser scanning data. *Remote sensing letters*, 7(3), 249–258.

Liu, R., Wang, P., Yan, Z., Lu, X., Wang, M., Yu, J., Tian, M., Ma, X., 2020. Hierarchical classification of pole-like objects in mobile laser scanning point clouds. *The Photogrammetric Record*, 35(169), 81–107.

Qin, R., Gruen, A., 2021. The role of machine intelligence in photogrammetric 3D modeling–an overview and perspectives. *International Journal of Digital Earth*, 14(1), 15–31.

Shi, Z., Kang, Z., Lin, Y., Liu, Y., Chen, W., 2018. Automatic recognition of pole-like objects from mobile laser scanning point clouds. *Remote Sensing*, 10(12), 1891.

Vaaja, M. T., Kurkela, M., Virtanen, J.-P., Maksimainen, M., Hyyppä, H., Hyyppä, J., Tetri, E., 2015. Luminance-corrected 3D point clouds for road and street environments. *Remote Sensing*, 7(9), 11389–11402.

Wang, R., 2013. 3D building modeling using images and LiDAR: A review. *International Journal of Image and Data Fusion*, 4(4), 273–292.

Wang, W., Fan, Y., Li, Y., Li, X., Tang, S., 2023. An Individual Tree Segmentation Method From Mobile Mapping Point Clouds Based on Improved 3-D Morphological Analysis. *IEEE Journal of Selected Topics in Applied Earth Observations and Remote Sensing*, 16, 2777–2790.

Wu, F., Wen, C., Guo, Y., Wang, J., Yu, Y., Wang, C., Li, J., 2016. Rapid localization and extraction of street light poles in mobile LiDAR point clouds: A supervoxel-based approach. *IEEE Transactions on Intelligent Transportation Systems*, 18(2), 292–305.

Yadav, M., Khan, P., Singh, A. K., 2022. Identification of pole-like objects from mobile laser scanning data of urban roadway scene. *Remote Sensing Applications: Society and Environment*, 26, 100765.

Yang, J., Kang, Z., Akwensi, P. H., 2018. A skeleton-based hierarchical method for detecting 3-D pole-like objects from mobile LiDAR point clouds. *IEEE Geoscience and Remote Sensing Letters*, 16(5), 801–805.

Yu, Y., Li, J., Guan, H., Wang, C., Yu, J., 2014. Semiautomated extraction of street light poles from mobile LiDAR point-clouds. *IEEE Transactions on Geoscience and Remote Sensing*, 53(3), 1374–1386.

Zhang, W., Qi, J., Wan, P., Wang, H., Xie, D., Wang, X., Yan, G., 2016. An easy-to-use airborne LiDAR data filtering method based on cloth simulation. *Remote sensing*, 8(6), 501.